sciendo

*Transport and Telecommunication, 2023, volume 24, no. 4, 409–422*
*Transport and Telecommunication Institute, Lomonosova 1, Riga, LV-1019, Latvia*
*DOI 10.2478/ttj-2023-0032*

# OPTIMIZATION OF BROADBAND MICROSTRIP ANTENNA DEVICE FOR 5G WIRELESS COMMUNICATION SYSTEMS

***Islam Islamov***

*Department of Radio Engineering and Telecommunication, Azerbaijan Technical University*
*AZ1073, H. Javid ave. 25, Baku, Azerbaijan*
*icislamov@mail.ru*

The paper proposes a new method for finding the optimal design of complementary split ring resonator cells for a microstrip antenna, which makes it possible to purposefully optimize the parameters of resonator cells, which significantly improve the electrical characteristics of the antenna. This antenna is designed for cellular communication 5G. The proposed method combines a regression model using a deep network based on fully connected neural layers with a search based on the conditional optimization algorithm COBYLA to find the optimal design parameters of resonator cells. This approach fully automates the process of creating microstrip antennas with resonator cells based on metamaterials and makes it possible to find the parameters of complementary split ring resonator cells that provide the optimal operating mode as a whole and gives the maximum level of antenna radiation while maintaining the bandwidth. The small size of complementary split ring resonator cells opens up the possibility of using this peculiar configuration to create compact and efficient microstrip antennas.

**Keywords:** Optimization; Wireless Communications; Microstrip Antenna Devices; Electromagnetic Field; Radiation Patterns; Electrical Characteristics

## 1. Introduction

Antennas are one of the most common types of sensors in geoecological monitoring systems, allowing you to create an “interface” between the transmitter or receiver and the observed environment. Compared to other types of antennas, microstrip antennas are the most commonly used in modern monitoring systems, as their design is excellent for this application due to their flat geometry and small size, while also having inherent disadvantages, such as low gain and distribution of radiation in space.

For example, such antennas can be successfully used to implement the hybrid sounding method proposed in (Yan *et al.*, 2022) for detecting hidden metal-containing objects, such as underground cable lines, pipelines, etc. At the same time, by increasing the radiation frequency at which the locator will operate, it will be possible to achieve a significant increase in the accuracy of localization of shallow objects.

The use of metamaterials in the design of antennas is a topical area of research; this allows, while maintaining small dimensions, to maximize their performance by changing the values of the magnetic and dielectric constants of the antenna substrate. However, the geometry of the metamaterial cells and their arrangement make it inexpedient to develop analytically the equations of the resulting electromagnetic fields. Because of this, engineers are forced to design the structures of such antennas through computationally laborious electromagnetic modelling using the trial and error method (Wangyu *et al.*, 2021).

Metamaterials are materials with special physical properties that cannot be reproduced using natural materials, therefore they are quite popular means in modern high-tech areas and are often used in many areas, such as microwave invisibility cloaks, submarines that use stealth technology, innovative electronics, microwave components, filters, etc. (Hong *et al.*, 2017).

In addition, metamaterials, brought about by recent advances in science and technology, have led to significant advances in the control and use of waves, including electromagnetic, acoustic, and mechanical waves. Thanks to various studies of metamaterials, such properties as negative refraction, extremely high refractive index, control of amplitude, phase and polarization of waves became available. The characteristics and properties of these metamaterials have made possible amazing and unusual phenomena that cannot be found among natural materials. This has had a profound impact on various fields of research and technology, including electromagnetic engineering, nanophotonics, optics, materials science, solid state physics, semiconductor physics, acoustics, and elastic mechanics (Zhang *et al.*, 2017).

One of the most important applications is the development of compact, highly efficient antennas, which have become a reality through the use of metamaterials. By using metamaterials with unique properties, it becomes possible to create antennas with innovative features that standard materials cannot provide. One or more metamaterial layers can be used as a substrate or in addition to the antenna structure to enhance its capabilities. For example, if a compact antenna with low cost and high efficiency is desired, the best option would be an antenna using metamaterials, which can help increase the bandwidth and gain of small antennas. Another advantage is that metamaterials not only reduce the geometric dimensions of antennas, but can also increase the directivity of the signal. If the size of the antenna does not matter, the use of metamaterials provides an advantage over traditional antennas, since it allows you to get a large bandwidth (Kurvinen *et al.*, 2019).

In the last decade, metamaterials have been used as wave absorbers, and since then this area of research has attracted a lot of attention. In (Li *et al.*, 2021), brief information about the absorber cell for the microwave range based on metamaterials was presented.

Metamaterials that absorb electromagnetic waves are often used in the military industry, due to their good performance and low weight, which is important for this area. For example, in (Chu *et al.*, 2017), a metamaterial structure of a composite with excellent absorption characteristics of electromagnetic waves covering the entire X-band radar is presented, which was developed and manufactured by them in order to practically test the properties.

Of particular interest is the design of resonators in the form of open rings as key building blocks for creating efficient media with negative magnetic permeability ($\mu_{\text{eff}} < 0$) or "left" materials. (Yijing *et al.*, 2021) demonstrates the potential of including subwavelength (that is, very small) split ring resonators and complementary split ring resonator cells (CSRR) to create compact microstrip notch filters to suppress unwanted spurious bands in the microwave range.

Typically, metamaterial-based antennas are designed through multiple simulations, and by making multiple adjustments to the antenna parameters using trial and error, the required set of antenna characteristics can be obtained. The amount of time it will take to complete this procedure is completely unpredictable and is determined, apart from luck, to some extent by the experience of the designer. In many well-known cases, the use of finite-differentiation time-domain modeling or the finite element method has yielded solutions with optimal performance, only by trial and error, backed up by professional reasoning and empirical knowledge. However, this process is time consuming and expensive, and due to the variety of design parameters and analytical degrees of freedom, even almost similar designs can have different results of numerical simulation and practical testing.

Fortunately, data mining-based data analysis methods, which have been booming in recent years, can also be used to solve this problem. Deep Neural Network (DNN) ideas, developing machine learning methods based on biological neural networks and using deep (or hierarchical) learning, began to develop rapidly in the 2000s, although they were known earlier. Deep learning is one of the machine learning methods used for regression and classification on large amounts of complex data using the principles of human brain thinking. Thanks to advances in deep learning, it is now being applied in a wide variety of fields, and its results can be seen in many areas of the economy. The greatest advances so far have been made mainly in computer vision, natural language processing, voice recognition, and video signal processing, but recent research has emerged showing the great potential of deep learning to speed up antenna design.

It is assumed that machine learning will speed up the antenna design procedure, while ensuring high accuracy, minimizing possible errors, saving time and making it possible to predict the behavior of the antenna, increasing the efficiency of calculations, and reducing the number of required simulations (Manshari *et al.*, 2020; He *et al.*, 2018, 2020; Yu *et al.*, 2021), which explains why the relevance of this study.

For example, paper (Rodriguez-Cano *et al.*, (2020) discusses a deep learning based method to quickly develop structure-type conductive layer cells for X-band (8-12 *GHz*) applications, which are cells with a side of 12,8 *mm*. They consist of a bottom part consisting of a ground plane, a dielectric and a square-patterned electromagnetic wave absorber cell with an area of 16×16 pixels, each pixel being a square with a 0,8 *mm* edge. The performance of such a cell depends on how the pixel square pattern is designed.

## 2. Formulation of the problem

Thus, the designs of microstrip antennas are widely described in the literature and give good results in practice. However, since they are inherently low-efficiency and limited in bandwidth, it is often necessary to optimize the design by reducing its geometry and improving its performance to meet the requirements of its practical application.

One way to achieve this is through the use of metamaterials (materials with special electrical characteristics). The geometry of the cells of the metamaterial and their array makes the analytical development of the resulting equations of the electromagnetic field very complicated and impractical. Traditionally, this problem has been solved by designing the antenna with many computationally expensive and time-consuming electromagnetic simulations. With the advent of available data processing libraries using deep neural networks and their hardware support, it became possible to optimize antenna designs by developing appropriate deep machine learning models, which avoids manual search for the optimal design and is the main aim of this study.

## 3. Research methods

*A. Features of microstrip antennas*

An antenna is a transitional structure between free space and a transmitting or receiving device. This last device is commonly referred to as a transmission line and is commonly known as a waveguide or feeder in telecommunication systems. Transmission lines can take the form of a coaxial cable or a hollow metal box and are used to transmit electromagnetic wave energy from a source to an antenna or from an antenna to a receiver. In the first case, we mean the transmitting antenna, and in the second case, the antenna receiving the signal. To describe the operation of an antenna, many parameters must be defined. Some of these parameters are interrelated and not all of them need to be specified to fully describe the performance of the antenna.

The radiation pattern of an antenna is defined as a mathematical function or graphical representation of the properties of an antenna in coordinate space. These properties may include radiation intensity and density, field strength, directivity, phase, or polarization. It is also important to note that these properties are usually normalized based on their maximum possible value, which can be expressed on a logarithmic scale or in decibels. This plot usually contains lobes, which are closed field concentrations, usually symmetrical. If an antenna has only one lobe of constant radius in all directions, the antenna is said to be isotropic or non-directional, meaning it radiates the same power regardless of direction.

Another important parameter is the radiation intensity $U$, defined as the power radiated by the antenna per unit solid angle in a given direction. This parameter can be obtained as follows

$$U = r^2 W_{rad}, \tag{1}$$

where $r$ is the distance; $W_{rad}$ is the radiation density.

It is also important to note that the antenna has a radiation efficiency $\eta_r$:

$$\eta_r = \frac{P_{rad}}{P_0}, \tag{2}$$

where $P_{rad}$ is the radiated power; $P_0$ is the power received by the antenna.

Directivity is a measure of an antenna's ability to concentrate radiated power in a particular direction. If the direction is not specified, then directivity is understood as the direction of maximum radiation intensity ($U = U_{max}$). This dimensionless measure can be represented mathematically through the equation:

$$D = \frac{U}{P_0} = \frac{4\pi U}{P_{rad}}. \tag{3}$$

The antenna gain $G$ is a measure of the ability to concentrate in a certain direction the power received by the antenna. This measure is also dimensionless and is more used in practice than directivity, since it is easier to measure the power received by an antenna than the power it radiates. It is defined as follows:

$$G = \eta_r D = \frac{4\pi U}{P_0}. \tag{4}$$

Theoretically, in the case of a lossless antenna ($\eta_r = 1$), directivity and gain will be the same. The bandwidth of an antenna is defined as the frequency range in which the characteristics of the antenna meet the specified standard in some respects. Bandwidth can be thought of as the range of frequencies on either side of the center frequency (usually the resonant frequency) where the characteristics of the antenna (such as input impedance, radiation pattern, beamwidth, polarization, sidelobe level, gain, beam direction,

radiation efficiency) are within the allowable value for the center frequency. For broadband antennas, the bandwidth is usually expressed as the ratio of high and low frequencies of acceptable performance. For example, a bandwidth of 10:1 means that the top frequency is 10 times the bottom frequency. For swept antennas, the bandwidth is expressed as a percentage of the frequency difference (top minus bottom) relative to the center frequency of the passband. For example, a bandwidth of 5% indicates that the frequency difference of acceptable performance is 5% of the center frequency of the bandwidth (Ozpinar *et al.*, 2020; Yongjian *et al.*, 2023).

The complex reflection coefficient $S_{11}$ shows how much of the incident high frequency power is reflected due to mismatch between the antenna and the feeder. The mismatch between the antenna and the feeder is the difference between the input impedance of the antenna and the characteristic impedance of the feeder or the impedance of the generator (if there is no transmission line). The dependence of the complex reflection coefficient on frequency makes it possible to determine the operating band of the antenna, which is taken from the amplitude level $S_{11} < -5$ *dB* (Janpangngern *et al.*, 2022; Nakano *et al.*, 2022).

As shown in Figure 1, microstrip antennas consist of a very thin metal strip called a patch, a dielectric layer also called a substrate, and a metal base called a ground plane. Substrate selection generally favors thin, low dielectric layers, specific characteristics may vary depending on the application. This choice takes into account the best value for money between antenna performance and construction cost.

The dielectric substrate in most cases should be electrically thin, and the dielectric constant should vary within $2{,}2 \leq \varepsilon_r \leq 12$. Patch antenna resonance is achieved when $L$ is close to $\lambda/2$. The input impedance is adjusted by changing the position of the feed point in the range from 50 to 300 Ohms (Sirous *et al.*, 2023), (Marin *et al.*, 2022).

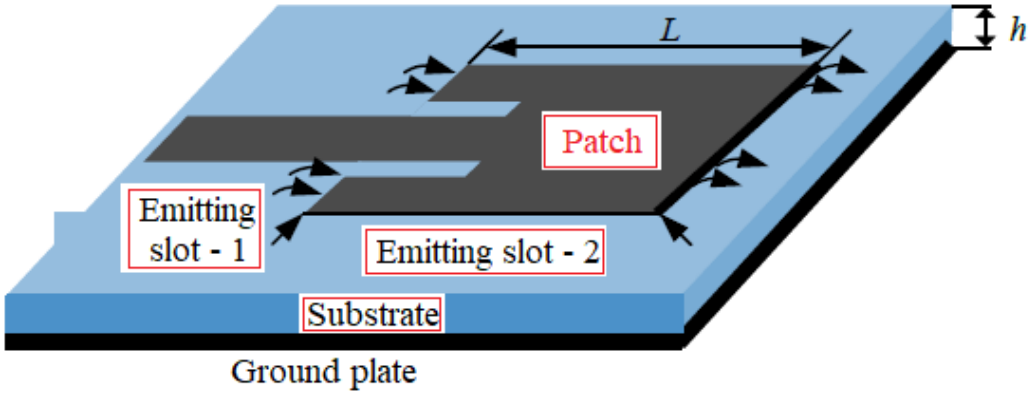



*Figure 1.* Microstrip antenna construction

*B. Initial data*

For definiteness, it is necessary to choose the resonant frequency of the microstrip antenna. The most promising, in our opinion, currently seems to be the 400 *MHz* band at 6 *GHz*, which can be used for use in the 5G cellular network. Or, for example, to determine the dielectric permittivity of rocks by the free space method (Minakshmi *et al.*, 2023). This range is currently not used in many countries (Zhenyu *et al.*, 2023) and is captured by available software-defined radio peripherals capable of transmitting or receiving radio signals in the range from 1 *MHz* to 6 *GHz*. For example, the HackRF One device, designed for testing and development of modern and radio technologies, is an open-source hardware platform that can be used as a USB peripheral or programmed for standalone operation (Wong *et al.*, 2021).

This program can be used to calculate many characteristics of an antenna, such as bandwidth, gain, return loss, etc. (Islamov *et al.*, 2018). Comparable functionality is provided by the Matlab Antenna Toolbox, although it can only use one CPU core for simulation, unlike CST MWS, which can use parallel processing on multiple CPU and GPU cores.

To improve the electrical characteristics, it is necessary to add metamaterial cells based on complementary open CSRR rings (Figure 2) with certain design parameters to the antenna design, as recommended in (Islamov *et al.*, 2018).

In Table 1 shows the values obtained by the method presented in (Mashhadi *et al.*, 2019). The simulated antenna is made of double-sided foil fiberglass with a foil thickness of 0.35 mm and a dielectric constant $\varepsilon_r = 4{,}3$ of size 61620 by 51480 $\mu m$, as recommended in (Boyuan *et al.*, 2021; Islamov *et al.*, 2019).

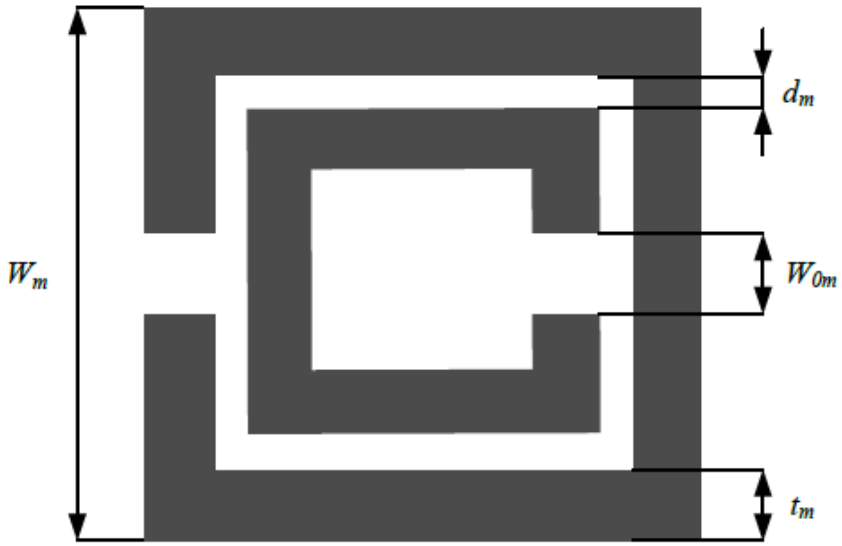



*Figure 2.* CSRR cell parameters: $W_m$ – CSRR cell height; $W_{0m}$ – ring clearance; dm is the distance between the rings; $t_m$ is the thickness of the rings; $X_a$ is the distance between the cell and the patch; $Y_a$ is the distance between cells; $R$ is the number of cells in the array on each side

Currently, only a small number of application software packages can be used to simulate the effects of metamaterials. A good example is the CST Microwave Studio (CST MWS) package.

**Table 1.** Design parameters of the microstrip antenna

| $L_e$, *mkm* | $W_e$, *mkm* | $W$, *mkm* | $L$, *mkm* | $h$, *mkm* | $W_0$, *mkm* | $y_0$, *mkm* | $g$, *mkm* |
|---|---|---|---|---|---|---|---|
| 61621 | 51481 | 23695 | 19821 | 1701 | 3505 | 6802 | 1003 |

Based on the rules of thumb proposed in work (Islamov *et al.*, 2019), the range of variation of these parameters is set is given as a function of the resonant wavelength $\lambda_0$:

$$\begin{cases} 0{,}025h_0 \le W_m \le \dfrac{\lambda_0}{4}, \\ t_m \approx 0{,}1W_m, \\ 0{,}0019\lambda_0 \le W_{0m} \le 0{,}0076\lambda_0, \\ 0{,}0009\lambda_0 \le d_m \le 0{,}0057\lambda_0. \end{cases} \tag{5}$$

The cells are located on the sides of the patch, as shown in Figure 3, taking into account antenna symmetry considerations. In order to cover a sufficient number of possible options, the intervals used when placing CSRR cells in an array are given by the equations:

$$\begin{cases} g \le X_a \le \left(\dfrac{W}{2} - \dfrac{W_m}{2}\right), \\ W_m \le Y_a \le \left(\dfrac{4L}{R-1} - W_m\right)0{,}1W_m, \\ R = 3,5,7. \end{cases} \tag{6}$$

Thus, the design parameters of CSRR cells can be specified by a tensor:

$$\overline{X} = \left[W_m, W_{0m}, d_m, t_m, R, X_a, Y_a\right] \tag{7}$$

Based on the above limits of change in the design parameters of CSRR cells, given by formulas (5), (6) in the CST MWS program in (Islamov *et al.*, 2022), the initial data for training neural networks were generated in the amount of 572 samples available in the public domain (Islamov *et al.*, 2023).

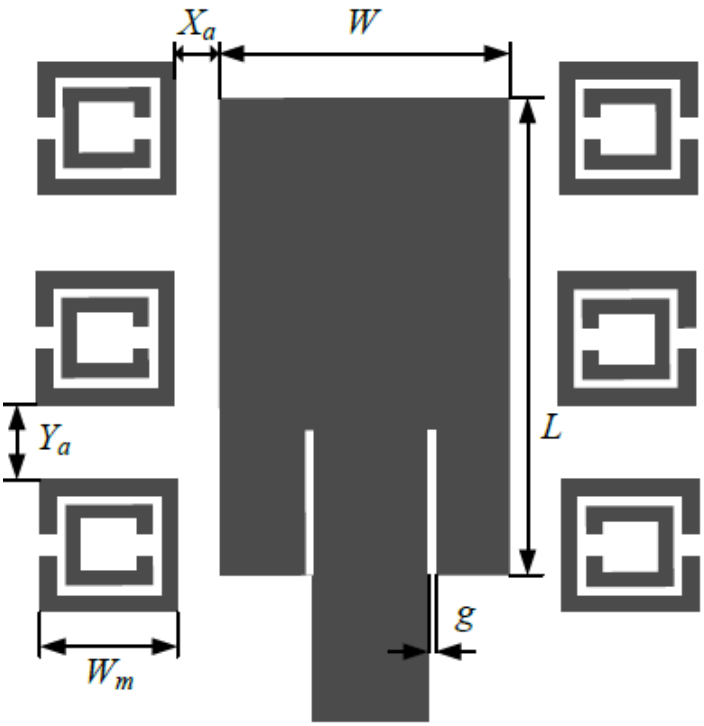



*Figure 3.* Location of CSRR cells relative to the antenna patch

To evaluate the electrical characteristics of the simulated electrical parameters of microstrip antennas with CSRR cells, using the CST MWS program, the following parameters were calculated:

$$\overline{Y} = \left[G_a, B_w, S_r\right], \tag{8}$$

where $G_a$ is the antenna gain, *dB*; $B_w$ is the bandwidth; $S_r$ is the return loss at the resonant frequency.

## 4. Method for optimizing design parameters resonator cells

A new method is proposed that makes it possible to optimize the parameters of the CSRR cells of the resonators, the mutual functioning of which will ensure the optimal operation of the antenna as a whole and will give the maximum radiation level of the antenna while maintaining the bandwidth. The proposed method combines a regression model using a deep network based on fully connected neural layers with a search based on a conditional optimization algorithm to find the best design parameters of resonator cells. This approach fully automates the process of creating microstrip antennas with resonator cells based on metamaterials and makes it possible to find the parameters of CSRR cells that give the best electrical characteristics of the antenna. In general terms, the method shown schematically in Figure 4 consists of two steps.

Step 1 is the training of the regressor network, which predicts the electrical characteristics of the antenna based on its design parameters, specified as a tensor of numbers. A tensor defining the parameters of the CSRR cells is fed into the neural network, and the network is trained to reduce the difference between the output predicted by the deep neural network and the corresponding electrical parameters of the antenna, obtained as a result of full numerical simulation in the CST MWS program.

Step 2 is the generation of new parameters of the CSRR cells of the resonators through iterative optimization. It combines the regressor network trained in step 1 with an optimization algorithm and uses some search strategy to find optimal CSRR cell parameters.

*A. Regressor network for determining the electrical characteristics of a microstrip antenna with SRR cells*

Well known, the task of regression is to predict the real label tensor from the available input data:

$$\hat{Y} = DDN(\overline{X}, \overline{Y}). \tag{9}$$

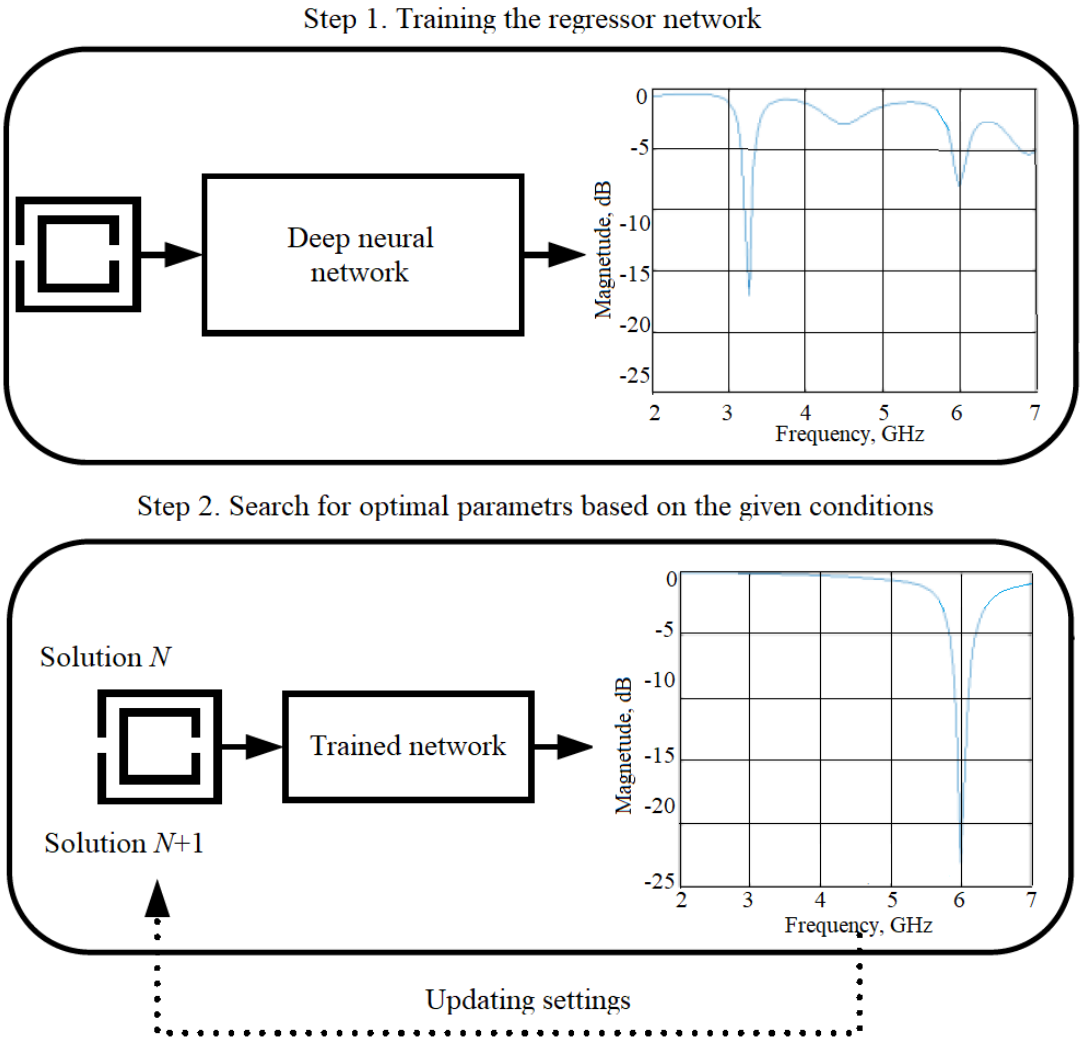



*Figure 4.* General scheme for searching for the optimal design of CSRR cells of a microstrip antenna

On Figure 5 shows the correlation matrix of the original data. Obviously, there is a correlation between $t_m$ and $W_m$ following from formula (5), and a negative correlation between the bandwidth $B_w$ and the return loss $S_r$. There is also a correlation between the bandwidth $B_w$ and the gain $G_a$.

It should be noted a significant positive correlation between the parameters $X_a$ and $B_w$, $Y_a$ and $S_r$, as well as a negative correlation between the parameters $X_a$ and $S_r$, $R$ and $S_r$. But still, the correlation between the parameters $G_a$, $B_w$ and $S_r$ is not complete and therefore it makes sense to use all three of these parameters for optimization.

Each feature in the source data has its own scale. For example, bandwidth is measured in megahertz, CSRR cell design parameters in micrometers, others in decibels, and so on. Well known, it is problematic to transfer values with very different ranges to a neural network.

The network, of course, will be able to automatically adapt to such heterogeneous data, but this will complicate training. In practice, it is customary to apply normalization to such data: for each feature in the input data, the average for this feature is subtracted from each value and the difference is divided by the standard deviation:

$$\begin{cases} \overline{\overline{Y}} = \dfrac{\overline{Y} - \langle \overline{Y} \rangle}{S(\overline{Y})}, \\ \overline{\overline{X}} = \dfrac{\overline{X} - \langle \overline{X} \rangle}{S(\overline{X})}. \end{cases} \tag{10}$$

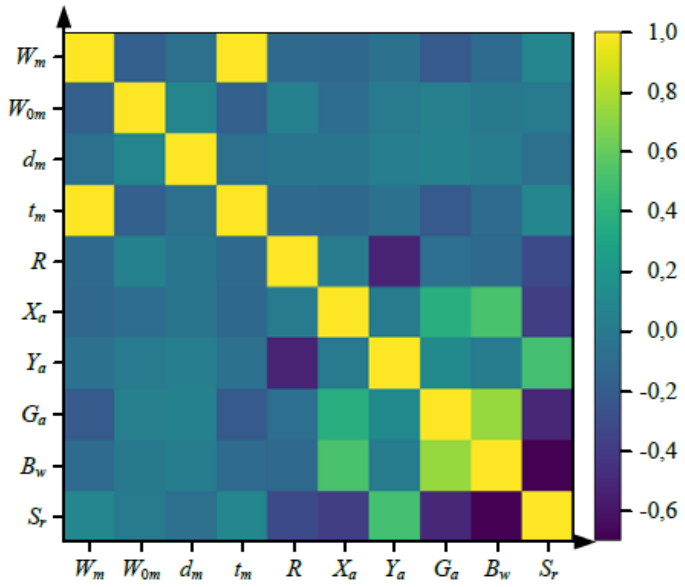



*Figure 5.* Input data correlation matrix

The input data is divided into training and control in a ratio of 4:1, and the values used to normalize the control data are calculated using only training to more accurately assess the quality of the trained neural network further.

Due to the small number of samples, a small network is used with three intermediate fully connected layers with 64 neurons each. This is due to the high computational complexity of numerical simulation in the CST MWS program, even despite the use of a GPU. Generally speaking, the less training data, the sooner overfitting is known to occur, and the use of a small network, the architecture of which is shown in Fig. 6 is one way to deal with it. In addition, the currently most popular method of combating overfitting is used, the so-called “decimation” with a factor of 0,1 after the first hidden layer.

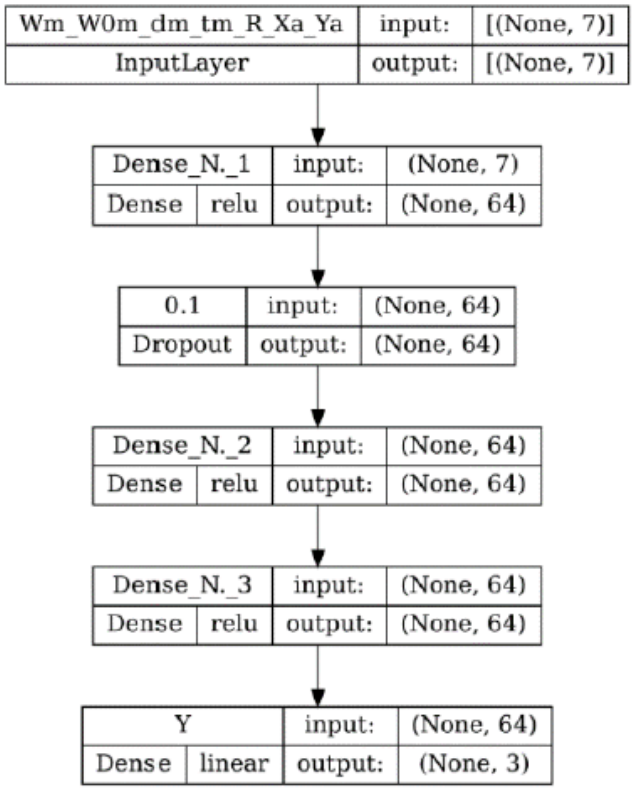



*Figure 6.* Regressor network architecture

Another more "accurate" way to deal with overfitting is to use $L_1$ regularization in the second fully connected layer, it is implemented in the proposed architecture by adding a penalty for increasing weights to the network loss function. The added penalty is directly proportional to the absolute values of the weight output coefficients, with proportionality factor $L_1 = 5 \cdot 10^{-4}$.

The network was trained with a loss function mse - mean sqeared error (mean square error), which calculates the square of the difference between the predicted and target values. This function is widely used in regression problems.

For a more convenient assessment of the network training results, the regression accuracy parameter mae - mean absolute error (mean absolute error) is used. This is the mean absolute value of the difference between predicted and target values.

To train the network, the Adam optimization algorithm was used with the initial learning rate $l_r = 10^3$, exponentially decreasing throughout the training with a constant coefficient $d_r = 0{,}95$ on packets of 32 samples.

The results of network training over 4000 epochs are shown in Figure 7.

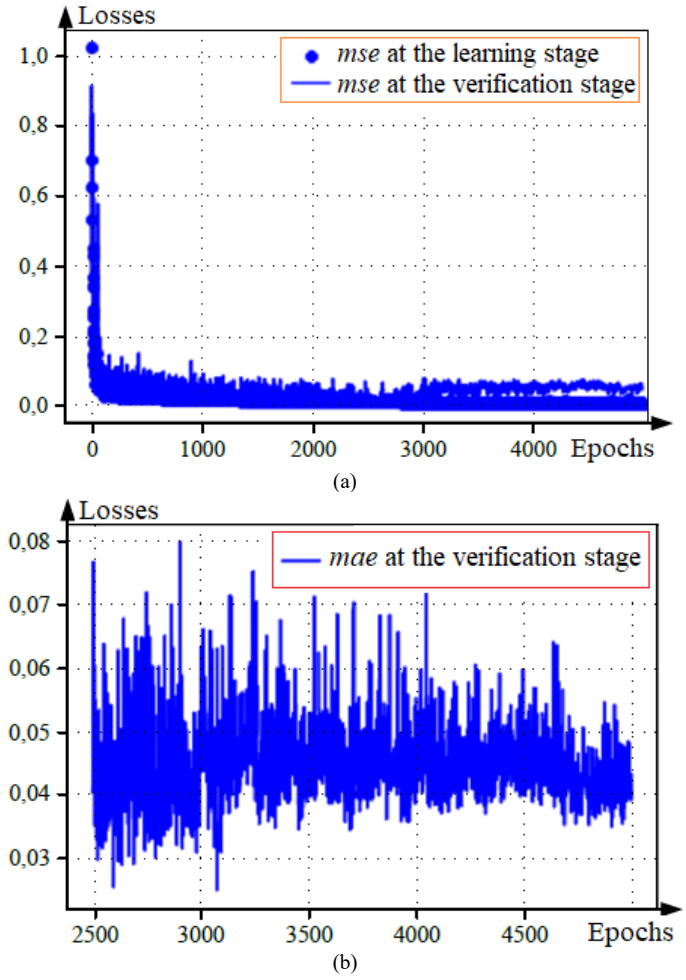



*Figure 7.* Changes in *mse* (a) and *mae* (b) during training of the regressor network

*B. Optimization of design parameters SRR-cells*

To determine the best design parameters of CSRR cells, it is proposed to define the function to be optimized as

$$A\left(\overline{\overline{Y}}\right) = k_g G_a + k_b B_w + k_s S_r, \tag{11}$$

where $k_g$, $k_b$, $k_s$ are weight coefficients reflecting the contribution of each parameter to the optimized function.

Then the optimization problem can be written as

$$A\left(\overline{\overline{Y}}\right) = \min_{\overline{X}}, \tag{12}$$

since the $\overline{\overline{Y}}$ values corresponding to $\overline{\overline{X}}$ cannot be directly calculated, a trained neural network is used to evaluate them, as suggested above.

$$\hat{\overline{Y}} = DNN\left(\overline{\overline{X}}\right). \tag{13}$$

Table 2 shows the parameters of CSRR cells obtained by solving the optimization problem (3) using the COBYLA method (Yu *et al.*, 2021) with additional restrictions imposed from geometric considerations:

$$\begin{cases} \overline{X}_i \geq 0,\ i = 1,2,3,...,7, \\ R \leq 8, \\ R(W_m + X_a) \leq L_g \end{cases} \tag{14}$$

and conditions (6) with weight coefficients equal to $k_g = -0{,}1$; $k_b = -0{,}1$; $k_s = 1$. That is, as a result of optimization, it is necessary to achieve a minimum return loss at the resonant frequency, while the resonant frequency of the CSRR cells will approximately coincide with one of the resonant frequencies of the microstrip antenna patch. In order not to worsen other electrical parameters of the antenna, the remaining weights should have small negative values.

**Table 2.** Optimal design parameters of CSRR cells

| $W_m$, *mkm* | $W_{0m}$, *mkm* | $d_m$, *mkm* | $t_m$, *mkm* | $R$ | $X_a$, *mkm* | $Y_a$, *mkm* | $S_r$ |
|---|---|---|---|---|---|---|---|
| 2244,5 | 295,9 | 743,6 | 224,5 | 5,3 | 8731,5 | 6948,9 | -25,5 |

## 5. Results and discussion

The results obtained in the simulation of microstrip antennas and experimental results are presented in Table 3, and in Fig. 8 shows the $S_{11}$ return loss curve in the 1-7 *GHz* band and antenna patterns at the resonant frequency of 6 *GHz*. The improvements can be explained by the fact that the CSRR cell is a very successful structure in which the capacitance between the two rings is combined with their inductance. A time-varying magnetic field with a strength vector perpendicular to the surface of the rings causes flows that, depending on the resonant properties of the substrate structure, generate a secondary electromagnetic field that either amplifies the original one or counteracts it, depending on the phase difference of the original and secondary electromagnetic waves.

**Table 3.** Comparative electrical characteristics of a microstrip antenna with and without CSRR cells

| Microstrip antenna without CSRR cells | | |
|---|---|---|
| | Theoretical | Experimental |
| Return Loss | -8,1 *dB* | -8,11 *dB* |
| Bandwidth ($S_{11}$<-5 *dB*) | ≈ 360 *MHz* | ≈ 360,1 *MHz* |
| Orientation | 6,1 *dB* | 6,12 *dB* |
| Microstrip antenna with optimum design CSRR cells | | |
| Return Loss | -23,2 *dB* | -23,22 *dB* |
| Bandwidth ($S_{11}$<-5 *dB*) | ≈ 360 *MHz* | ≈ 360,1 *MHz* |
| Orientation | 9,8 *dB* | 9,82 *dB* |

The resonant frequency obtained with two annular open-loop resonators must be much lower than that corresponding to classical annular or rectangular single-open-loop resonators of similar dimensions. This feature is due to the large distributed capacitance between the two rings. The small size of CSRR cells opens up the possibility of using this peculiar configuration to create compact microstrip antennas. Since there are many different parameters that affect the resonant frequency of CSRR cells, the most important of which are the permittivity of the substrate and the length of the resonator, we restrict ourselves to the numerical determination of the resonant frequency by simulation.

As can be seen from Fig. 9, the resonant frequency of the array of CSRR cells indeed coincides with the second resonant frequency of the microstrip antenna, which confirms the above hypothesis. The CSRR cell, acting as a structural element of the substrate metamaterial, together with other elements of the microstrip antenna forms local resonant subregions that change its effective magnetic permeability.

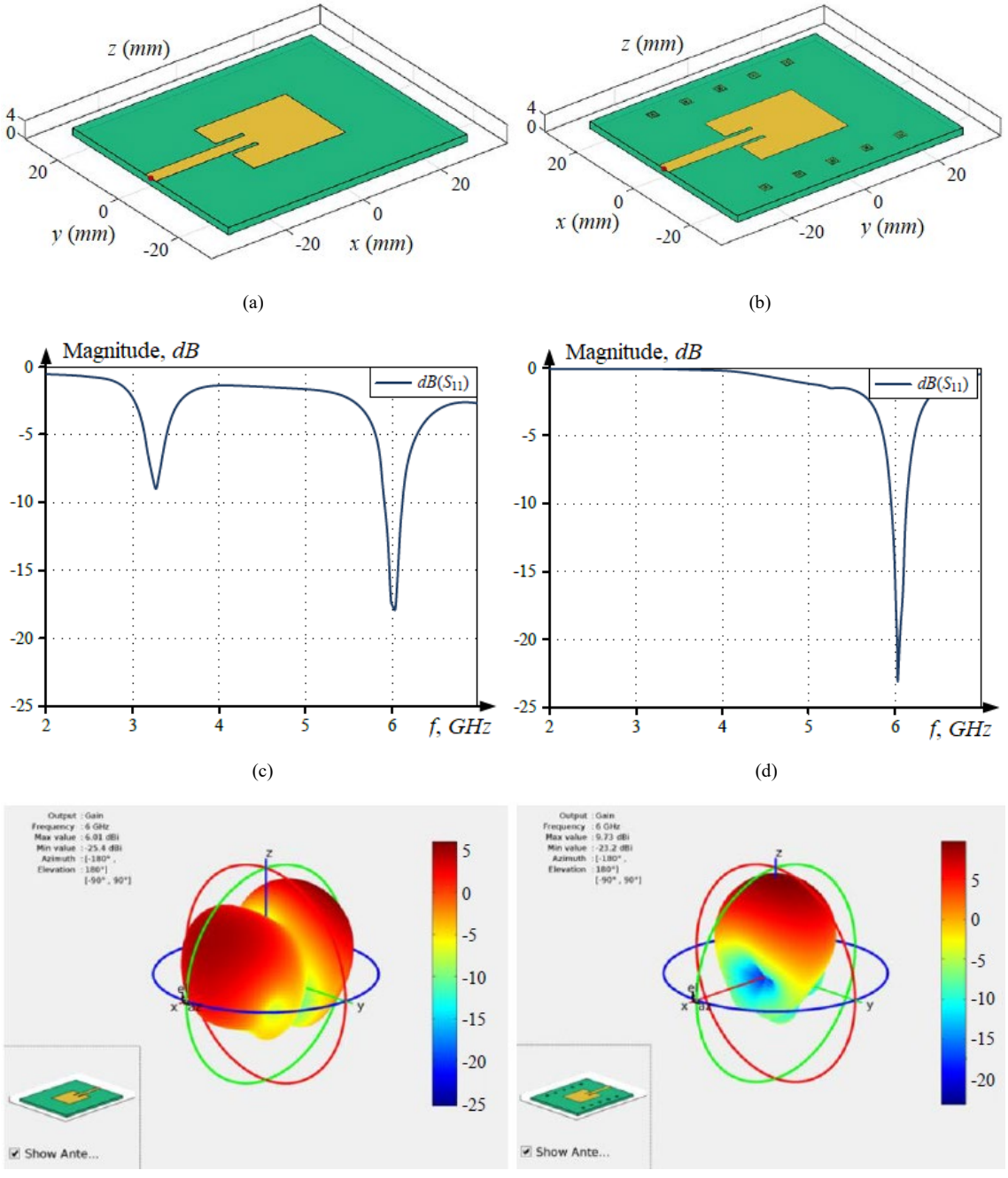
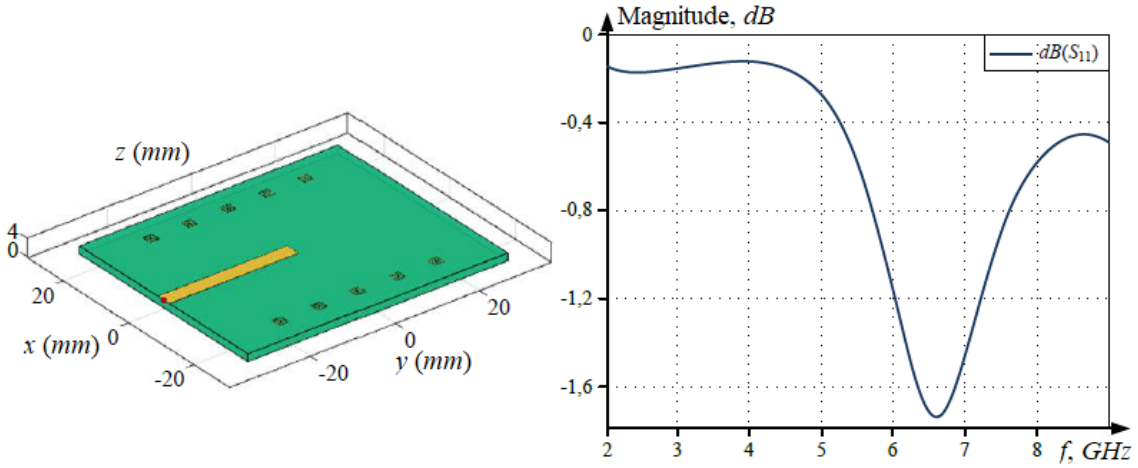


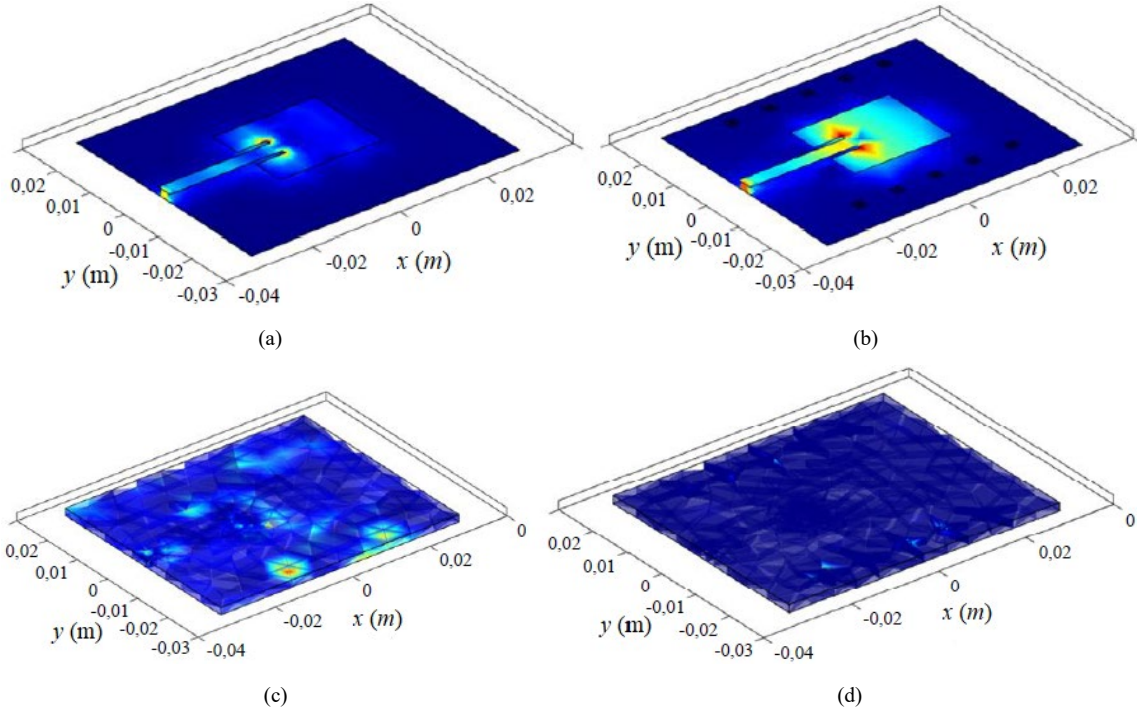

*Figure 8.* Electrical characteristics of a microstrip antenna and an antenna with CSRR cells: a, b – appearance; c, d – $S_{11}$ return loss curve; e, f - radiation pattern

The mutual functioning of these resonant regions ensures the optimal operation of the antenna as a whole and gives the maximum radiation level of the antenna while maintaining the bandwidth, which is confirmed by the current distribution in the antenna elements shown in Fig. 10. In this case, the current is redistributed between the substrate and the antenna patch towards the patch, which explains the obtained improvements in the electrical characteristics of the antenna.




(a) (b)

*Figure 9.* CSRR cell appearance (a) and return loss curve (b)




(a) (b)

(c) (d)

*Figure 10.* Current distribution: a, b - in the antenna elements; c, d – in the dielectric of the substrate

## 6. Conclusions

Thus, antennas are one of the most common types of sensors in geoecological monitoring systems, allowing you to create an "interface" between the transmitter or receiver and the environment under study. Microstrip antenna designs are widely described in the literature and give good results in practice, but they themselves are characterized by low efficiency and limited bandwidth, so it is necessary to optimize the design by changing its parameters and improving the technical characteristics to meet the requirements of its practical application. One way to achieve this is through the use of metamaterials. Metamaterials are materials with remarkable electrical characteristics. However, the features of the metamaterial cells and their array make the analytical development of the resulting equations of the electromagnetic field very complicated and impractical. Traditionally, this problem has been solved by designing the antenna with many computationally expensive and time-consuming electromagnetic simulations. With the advent of available data processing libraries using deep neural networks and their hardware support, it became possible to optimize antenna designs by developing appropriate deep machine learning models, which avoids manual search for the optimal design.

Therefore, in this paper, we propose a new method for finding the optimal design of CSSR cells for a microstrip antenna, which makes it possible to purposefully optimize the parameters of resonator cells, which significantly improve the electrical characteristics of the antenna. The proposed method combines a regression model using a deep network based on fully connected neural layers with a search based on the conditional optimization algorithm COBYLA to find the optimal design parameters of resonator cells. This approach fully automates the process of creating microstrip antennas with resonator cells based on metamaterials and makes it possible to find the parameters of CSRR cells that provide the optimal operating mode as a whole and gives the maximum level of antenna radiation while maintaining the bandwidth. The small size of CSRR cells opens up the possibility of using this peculiar configuration to create compact and efficient microstrip antennas.

## Acknowledgements

The author would like to thank the editor and anonymous reviewers for constructive, valuable suggestions and comments on the work.

## References

1. Boyuan, M., Pan, J., Huang, S., Yang, D., and Guo, Y. (2021) Wide-beam dielectric resonator antennas based on the fusion of higher-order modes. *IEEE Trans. Antennas Propag*., 69(12), 8866-8871.
2. Chu, H., and Guo, Y.-X. (2017) A filtering dual-polarized antenna subarray targeting for base stations in millimeter-wave 5G wireless communications. *IEEE Trans. Compon. Package. Manuf. Technol*., 7(6), 964-973.
3. He, Y., and Li, Y. (2020) Dual-polarized microstrip antennas with capacitive via fence for wide beamwidth and high isolation. *IEEE Trans. Antennas Propag*., 68(7), 5095-5103.
4. He, Y., Li, Y., Sun, W., Zhang, Z., and Chen, P.-Y. (2018) Dual linearly polarized microstrip antenna using a slot-loaded TM 50 mode. *IEEE Antennas Wireless Propag. Lett*., 17(12), 2344-2348.
5. Hong, W., Baek K.-H., and Ko S. (2017) Millimeter-wave 5G antennas for smartphones: Overview and experimental demonstration, *IEEE Trans. Antennas Propag*., 65(12), 6250-6261.
6. Islamov, I. J., and Ismibayli, E. G. (2018) Experimental Study of Characteristics of Microwave Devices Transition from Rectangular Waveguide to the Megaphone. *IFAC-PapersOnLine*, 51(30), 477-479.
7. Islamov, I. J., Hunbataliyev, E. Z., and Zulfugarli, A. E. (2022) Numerical Simulation of Characteristics of Propagation of Symmetric Waves in Microwave Circular Shielded Waveguide with a Radially Inhomogeneous Dielectric Filling. *International Journal of Microwave and Wireless Technologies*, 9, 761-767.
8. Islamov, I. J., Ismibayli, E. G., Gaziyev, Y. G., Ahmadova, S. R., and Abdullayev, R. Sh. (2019) Modeling of the Electromagnetic Feld of a Rectangular Waveguide with Side Holes. *Progress in Electromagnetics Research*, 81, 127-132.
9. Islamov, I. J., Ismibayli, E. G., Hasanov, M. H., Gaziyev, Y. G., and Abdullayev, R Sh. (2018) Electrodynamics Characteristics of the No Resonant System of Transverse Slits Located in the Wide Wall of a Rectangular Waveguide. *Progress in Electromagnetics Research Letters*, 80, 23-29.
10. Islamov, I. J., Ismibayli, E. G., Hasanov, M. H., Gaziyev, Y. G., Ahmadova, S. R., and Abdullayev, R. Sh. (2019) Calculation of the Electromagnetic Field of a Rectangular Waveguide with Chiral Medium. *Progress in Electromagnetics Research*, 84, 97-114.
11. Islamov, I., and Safarli, A. (2023) Design, Modelling and Research of an Antenna System for Transmitting and Receiving Information in Satellite Systems. *Transport and Telecommunication*, 24(3), 297-308.
12. Janpangngern, P., Torrungrueng, D., Krairiksh, M., and Phongcharoenpanich, C. (2022) Dual-band circularly polarized omni-directional biconical antenna with double-circular parallelepiped elements for WLAN applications. *IEEE Access*, 10, 31970-31980.
13. Kurvinen, J., Kahkonen, H., Lehtovuori, A., Ala-Laurinaho, J., and Viikari, V. (2019) Co-designed mm-wave and LTE handset antennas. *IEEE Trans. Antennas Propag*., 67(3), 1545-1553.
14. Li, H., Li, Y., Chang, L., Sun, W., Qin, X., and Wang, H. (2021) A wideband dual-polarized endfire antenna array with overlapped apertures and small clearance for 5G millimeter-wave applications. *IEEE Trans. Antennas Propag*., 69(2), 815-824.
15. Manshari, S., Koziel, S., and Leifsson, L. (2020) Compact dual-polarized corrugated horn antenna for satellite communications. *IEEE Trans. Antennas Propag*., 68(7), 5122-5129.
16. Marin, J. G., Baba, A. A., Hesselbarth, J., Hashmi, R. M., and Esselle, K. P. Millimeter-wave low-loss multifeed superstrate-based antenna. *IEEE Trans. Antennas Propag*., 68(5), 3387-3396.

17. Mashhadi, S., Jiao, Y., and Chen, J. (2019) Broadbeam cylindrical dielectric resonator antenna. *IEEE Access*, 7, 112653-112661.
18. Minakshmi, S., and Yogesh, K. C. (2023) Reconfigurable polarization and pattern microstrip antenna for IRNSS band applications. *AEU - International Journal of Electronics and Communications*, 160, 154501.
19. Nakano, H., Abe, T., and Yamauchi, J. (2022) A small metaline array antenna for circularly polarized dual-band beam-steering. *IEEE Access*, 10, 73317-73325.
20. Ozpinar, H., Aksimsek, S., and Tokan, N. T. (2020) A novel compact broadband high gain millimeter-wave antenna for 5G beam steering applications. *IEEE Trans. Veh. Technol*., 69(3), 2389-2397.
21. Rodriguez-Cano, R., Zhao, K., Zhang, S., and Pedersen, G. F. (2020) Handset frame blockage reduction of 5G mm-Wave phased arrays using hard surface inspired structure. *IEEE Trans. Veh. Technol*., 69(8), 8132-8139.
22. Sirous, B., Dongseop, L., Wonbin, H., and Ho-Jin, S. (2023) Analysis of On-Antenna Power Combining for Realization of Pattern-Reconfigurable Multifeed Microstrip Antennas. *IEEE Transactions on Antennas and Propagation*, 71(4), 3091-3103.
23. Wangyu, S., Yue, L., Le, C., Hao, L., Xu, Q., and Hanyang, W. (2021) Dual-Band Dual-Polarized Microstrip Antenna Array Using Double-Layer Gridded Patches for 5G Millimeter-Wave Applications. *IEEE Transactions on Antennas and Propagation*, 69(10), 6489-6499.
24. Wong, K., Chen, C., and Li, W. (2021) Integrated four low-profile shorted patch dual-band WLAN MIMO antennas for mobile device applications. *IEEE Trans. Antennas Propag*., 69(6), 3566-3571.
25. Yan, X., Wen, J., Kun, W., Tao, H., Tong, C., and Shuxi, G. (2022) Wideband RCS Reduction of Microstrip Antenna Array Using Coding Metasurface with Low Q Resonators and Fast Optimization Method. *IEEE Antennas and Wireless Propagation Letters*, 21(4), 656-660.
26. Yijing, H., and Yue, L. (2021) Compact Co-Linearly Polarized Microstrip Antenna with Fence-Strip Resonator Loading for In-Band Full-Duplex Systems. *IEEE Transactions on Antennas and Propagation*, 69(11), 7125-7133.
27. Yongjian, Z., Yue, L., Mingzhe, H., Pengfei, W., and Hanyang, W. (2023) Dual-Band Circular-Polarized Microstrip Antenna for Ultrawideband Positioning in Smartphones with Flexible Liquid Crystal Polymer Process. *IEEE Transactions on Antennas and Propagation*, 71(4), 3155-3163.
28. Yu, Q. G., Yong, M. P., Shao, Y. Z., and Kai, L. (2021) A Singly-Fed Dual-Band Microstrip Antenna for Microwave and Millimeter-Wave Applications in 5G Wireless Communication. *IEEE Transactions on Vehicular Technology*, 70(6), 5419-5430.
29. Zhang, J., Ge, X., Li, Q., Guizani M., and Zhang Y. (2017) 5G millimeter-wave antenna array: Design and challenges. *IEEE Wireless Commun*., 24(2), 106-112.
30. Zhenyu, L., Yijing, H., and Yue, L. (2023) Beamwidth Enhancement of Microstrip Antennas Using Capacitive Via-Fence Loading. *IEEE Open Journal of Antennas and Propagation*, 4, 151-158.